Control Strategy for Flexible Microgrid Based on Parallel Line-Interactive UPS Systems

Josep M. Guerrero, *Senior Member, IEEE*, Juan C. Vásquez, José Matas, Miguel Castilla, and Luis García de Vicuña

***Abstract*—In this paper, the control strategy for a flexible microgrid is presented. The microgrid presented here consists of several line-interactive uninterruptible power supply (UPS) systems connected in parallel. The control technique is based on the droop method to avoid critical communications among UPS units. Thus, a flexible microgrid is obtained to operate in either grid-connected or islanded mode. A small-signal analysis is presented in order to analyze the system stability, which gives rules to design the main control parameters. Simulation and experimental results are presented, showing the feasibility of the proposed controller.**

***Index Terms*—Distributed generation (DG), droop method, microgrids, uninterruptible power systems.**

I. Introduction

MICROGRIDS are becoming a reality in a scenario in which renewable energy, distributed generation (DG), and distributed storage systems can be conjugated and integrated into the grid. These concepts are growing due not only to environmental aspects but also to social, economical, and political interests. The variable nature of some renewable energy systems, such as photovoltaic (PV) or wind energy, relies on natural phenomenon, such as sunshine or wind. Consequently, it is difficult to predict the power that can be obtained through these prime sources, and the peaks of power demand do not coincide necessarily with the generation peaks. Hence, storage energy systems are required if we want to supply the local loads in an uninterruptible power supply (UPS) fashion [1], [2], [31], [32]. Some small and distributed energy storage systems can be used for this purpose, such as flow batteries, fuel cells, flywheels, superconductor inductors, or compressed air devices.

The DG concept is growing in importance, pointing out that the future utility line will be formed by distributed energy resources and small grids (minigrids or microgrids) interconnected between them [23], [24]. In fact, the responsibility of the final user is to produce and store part of the electrical power of the whole system. Hence, microgrid can export or import energy to the utility through the point of common coupling (PCC). Moreover, when there is utility failure, the microgrid can still work as an autonomous grid. As a consequence, these two classical applications, namely, grid-connected and islanded operations, can be used in the same application. In this sense, the droop control method is proposed as a good solution to connect, in parallel, several inverters in an island mode [4]–[7]. However, although it has been investigated and improved, this method by itself is not suitable for the coming flexible microgrids. Further, although there are line-interactive UPSs in the market, still, there are no line-interactive UPS systems able to operate in parallel autonomously, forming a microgrid [25], [26].

In this paper, a control scheme for UPSs connected in parallel, forming a microgrid, is proposed. The microgrid presented in this paper is formed by parallel-connected UPS inverters. Its difference from the conventional parallel UPS systems [27]–[29] is that the flexible microgrid can not only import and export energy to the main grid but also can operate in grid-connected or in island modes. The presented application is a PV system with 6-kVA line-interactive UPS units [30]. The typical applications of these PV-UPS systems are domestic, up to 30 kVA. The UPS inverters use a droop control function in order to avoid critical communication between the modules. The droop function can manage the output power of each UPS as a function of the battery charge level. The inverters, compared with the conventional methods, act as voltage sources even when they are connected to the grid [21], [22]. In this situation, they are able to share power with the grid, based on its nominal power. Finally, the intelligent static bypass switch connects or disconnects the microgrid and sends proper references to the local UPS controllers by means of low bandwidth communications.

This paper is organized as follows. In Section II, we describe all the hierarchical control of a microgrid structure. In Section III, we review the basic of the droop control method and the power-flow analysis. In Section IV, the control of the microgrid and the different operation modes are explained. Section V shows the UPS control, including the virtual output impedance and the power-sharing loops. Section VI develops a small-signal analysis that is used for the proper design of the control parameters. Section VII shows the microgrid simulation and experimental results. In Section VIII, the conclusions of this paper are given.

II. Microgrid Structure and Control

A flexible microgrid has to be able to import/export energy from/to the grid, control the active and reactive-power flows, and manage the energy storage. Fig. 1 shows a microgrid,

Manuscript received February 29, 2008; revised October 15, 2008. First published November 18, 2008; current version published February 27, 2009. This work was supported by the Spanish Ministry of Science and Technology under Grant ENE2006-15521-C03-01.

J. M. Guerrero and J. C. Vásquez are with the Department of Automatic Control Systems and Computer Engineering, Technical University of Catalonia, 08036 Barcelona, Spain (e-mail: josep.m.guerrero@upc.edu; juan.carlos.vasquez@upc.edu).

J. Matas, M. Castilla, and L. García de Vicuña are with the Department of Electronic Engineering, Technical University of Catalonia, 08800 Vilanova i la Geltrú, Spain (e-mail: matasalc@gmail.com; mcastilla@eel.upc.edu; vicuna@eel.upc.edu).

Color versions of one or more of the figures in this paper are available online at http://ieeexplore.ieee.org.

Digital Object Identifier 10.1109/TIE.2008.2009274

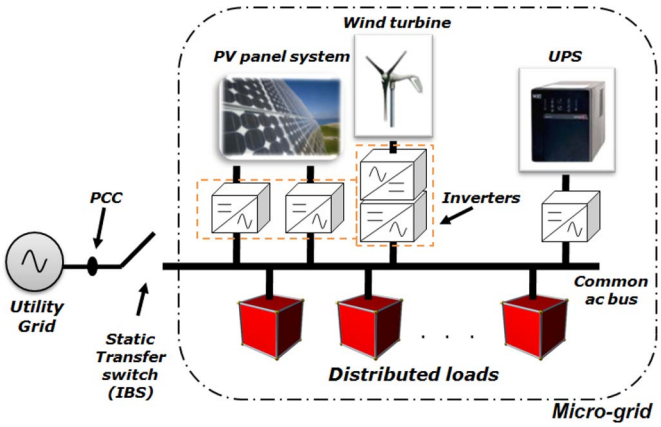

Fig. 1. Diagram of a flexible microgrid.

including small generators, storage devices, and local critical and noncritical loads, which can operate both, connected to the grid or autonomously in island mode. This way, the power sources (PV arrays, small wind turbines, or fuel cells) or storage devices (flywheels, superconductor inductors, or compressed-air systems) use electronic interfaces between them and the microgrid. Usually, these interfaces are ac/ac or dc/ac power electronic converters, also called inverters.

Traditionally, inverters have two separate operation modes acting as a current source, if they are connected to the grid, or as a voltage source, if they work autonomously. In this last case, the inverters must be disconnected from the grid when a grid fault occurs, for security reasons and to avoid islanding operation. However, if we want to impulse the use of decentralized generation of electrical power, the DG, and the implantation of the microgrids, islanding operation should be accepted if the user is completely disconnected from the grid. In this case, the microgrid could operate as an autonomous grid, using the following three control levels.

1) *Primary control*. The inverters are programmed to act as generators by including virtual inertias through the droop method, which ensures that the active and the reactive powers are properly shared between the inverters.
2) *Secondary control*. The primary control achieves power sharing by sacrificing frequency and amplitude regulation. In order to restore the microgrid voltage to nominal values, the supervisor sends proper signals by using low bandwidth communications. This control also can be used to synchronize the microgrid with the main grid before they have to be interconnected, facilitating the transition from islanded to grid-connected mode.
3) *Tertiary control*. The set points of the microgrid inverters can be adjusted, in order to control the power flow, in global (the microgrid imports/exports energy) or local terms (hierarchy of spending energy). Normally, the power-flow priority depends on economic issues. Economic data must be processed and used to make decisions in the microgrid.

Fig. 1 shows the schematic diagram of a microgrid. In our example, it consists of several PV strings connected to a set of line-interactive UPSs forming a local *ac* microgrid, which can be connected to the utility mains through an intelligent bypass switch (IBS). The IBS is continuously monitoring its both sides, namely, the mains and the microgrid. If there is a fault in the mains, the IBS will disconnect the microgrid from the grid, creating an energetic island. When the main is restored, all UPS units are advised by the IBS to synchronize with the mains to properly manage the energy reconnection.

The microgrid has two main possible operation modes: grid-connected and islanded modes. The transitions between both modes and the connection or disconnection of UPS modules should be made seamlessly (hot-swap or plug-and-play capabilities) [8]–[11]. In this sense, the droop control method has been proposed for islanding microgrids [3]. Taking into account the features and limitations of the droop method, we propose a control structure for a microgrid which could operate in both grid-connected and islanded modes. The operation of the inverters is autonomous, contrary to other microgrid configurations [27]–[29] which use master–slave principles. Only low bandwidth communications are required in order to control the microgrid power flow and synchronization with the utility grid.

III. Droop-Method Concept

With the aim of connecting several parallel inverters without control intercommunications, the droop method is often proposed [12]. The applications of such a kind of control are typically industrial UPS systems [13] or islanding microgrids [14], [15]. The conventional droop method is based on the principle that the phase and the amplitude of the inverter can be used to control active and reactive-power flows [16]. Hence, the conventional droop method can be expressed as follows:

$$\omega = \omega^* - mP \tag{1}$$
$$E = E^* - nQ \tag{2}$$

where E is the amplitude of the inverter output voltage; ω is the frequency of the inverter; ω^* and E^* are the frequency and amplitude at no-load, respectively; and m and n are the proportional droop coefficients. The active and reactive powers flowing from an inverter to a grid through an inductor can be expressed as follows [17]:

$$P = \left(\frac{EV}{Z}\cos\phi - \frac{V^2}{Z}\right)\cos\theta + \frac{EV}{Z}\sin\phi\sin\theta \tag{3}$$
$$Q = \left(\frac{EV}{Z}\cos\phi - \frac{V^2}{Z}\right)\sin\theta - \frac{EV}{Z}\sin\phi\cos\theta \tag{4}$$

where Z and θ are the magnitude and the phase of the output impedance, respectively; V is the common bus voltage; and ϕ is the phase angle between the inverter output and the microgrid voltages. Notice that there is no decoupling between $P-\omega$ and $Q-E$. However, it is very important to keep in mind that the droop method is based on two main assumptions.

Assumption 1: The output impedance is purely inductive, and $Z = X$ and $\phi = 90^\circ$ with (3) and (4) become

$$P = \frac{EV}{X}\sin\phi \tag{5}$$
$$Q = \frac{EV}{X}\cos\phi - \frac{V^2}{X}. \tag{6}$$

This is often justified due to the large inductor of the filter inverter and to the impedance of the power lines. However, the inverter output impedance depends on the control loops, and the impedance of the power lines is mainly resistive in low-voltage applications. This problem can be overcome by adding an output inductor, resulting in an LCL output filter, or by programming a virtual output impedance through a control loop.

Assumption 2: The angle ϕ is small; we can derive that $\sin\phi \approx \phi$ and $\cos\phi \approx 1$, and consequently,

$$P \approx \frac{EV}{X}\phi \tag{7}$$

$$Q \approx \frac{V}{X}(E - V). \tag{8}$$

Note that, taking into account these considerations, P and Q are linearly dependent on ϕ and E. This approximation is true if the output impedance is not too large, as in most practical cases.

In the droop method, each unit uses frequency instead of phase to control the active-power flows, considering that they do not know the initial phase value of the other units. However, the initial frequency at no load can be easily fixed as ω^*. As a consequence, the droop method has an inherent tradeoff between the active-power sharing and the frequency accuracy, thus resulting in frequency deviations. In [18], frequency restoration loops were proposed to eliminate these frequency deviations. However, in general, it is not practical, since the system becomes unstable due to inaccuracies in inverters' output frequency, which leads to increasing circulating currents.

IV. Microgrid Control

The aim of this section is to develop a flexible control that can operate in grid-connected and islanded operations and to enable the transition between both modes.

A. Grid-Connected Operation

In this mode, the microgrid is connected to the grid through an IBS. In this case, all UPSs have been programmed with the same droop function [14], [18]

$$\omega = \omega^* - m(P - P^*) \tag{9}$$

$$E = E^* - n(Q - Q^*) \tag{10}$$

where P^* and Q^* are the desired active and reactive powers. Normally, P^*should coincide with the nominal active power of each inverter, and $Q^* = 0$.

However, we have to distinguish between two possibilities: 1) importing energy from the grid or 2) exporting energy to the grid. In the first scenario, in which the total load power is not fully supplied by the inverters, the *IBS* must adjust P^* by using low bandwidth communications to absorb the nominal power from the grid in the PCC.

This is done with small increments and decrements of P^* as a function of the measured grid power, by using a slow PI controller, as follows:

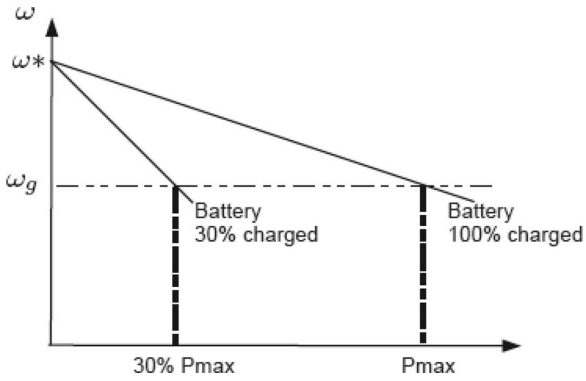

Fig. 2. Droop characteristic as a function of the batteries' charge level.

$$P^* = k_p\left(P_g^* - P_g\right) + k_i \int \left(P_g^* - P_g\right) dt + P_i^* \tag{11}$$

where P_g and P_g^* are the measured and the reference active powers of the grid, respectively, and P_i^* is the nominal power of the inverter i. This way, the UPSs with a low battery level can switch to charger mode by using $P^* < 0$. Similarly, we proposed that reactive-power control law can be defined as

$$Q^* = k_p'\left(Q_g^* - Q_g\right) + k_i' \int \left(P_g^* - P_g\right) dt + Q_i^* \tag{12}$$

where Q_g and Q_g^* are the measured and the reference reactive powers of the grid, respectively, and Q_i^* is the nominal reactive power.

The second scenario occurs when the power of the prime movers (e.g., PV panels) is much higher than those required by the loads and when the batteries are fully charged. In this case, the *IBS* may enforce to inject the rest of the power to the grid. Moreover, the *IBS* has to adjust the power references.

B. Islanded Operation

When the grid is not present, the *IBS* disconnects the microgrid from the main grid, starting the autonomous operation. In such a case, the droop method is enough to guarantee proper power sharing between the UPSs. However, the power sharing should take into account the batteries' charging level of each module. In this case, the droop coefficient m can be adjusted to be inversely proportional to the charge level of the batteries, as shown in Fig. 2

$$m = \frac{m_{\min}}{\alpha} \tag{13}$$

where $m_{\min}$ is the droop coefficient at full charge and α is the level of charge of the batteries ($\alpha = 1$ is fully charged and $\alpha = 0.01$ is empty). The coefficient α is saturated to prevent m from rising to an infinite value.

C. Transitions Between Grid-Connected and Islanded Operations

When the *IBS* detects some fault in the grid, it disconnects the microgrid from the grid. In this situation, the *IBS* can

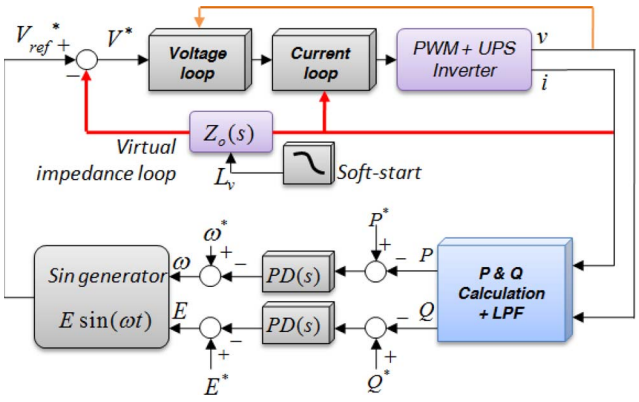

Fig. 3. Block diagram of the inverter control loops.

TABLE I
CONTROL SYSTEM PARAMETERS

Parameter	Symbol	Value	Units
Nominal frequency	ω^*	$2\pi \cdot 50$	rad/s
Nominal amplitude	E	311	V
Nominal virtual output impedance	$L_{Df}{}^*$	800	μH
Initial output impedance value	$L_{Do}{}^*$	80	mH
Soft-start time constant	T_{ST}	0.1	s
P Proportional term value	k_p	1.8	W^{-1}
P Integral term value	k_i	0.1	s/W
Q Proportional term value	k_p'	30	VAr^{-1}
Q Integral term value	k_i'	80	s/VAr

readjust the power reference to the nominal values; however, this action is not mandatory. Instead, the *IBS* can measure the frequency and the amplitude of the voltage inside the microgrid and move the set points (P^* and Q^*) in order to avoid the corresponding frequency and amplitude deviations of the droop method. In contrast, when the microgrid is working in islanded mode and the *IBS* detects that the voltage outside of the microgrid is stable and fault-free, the islanded mode can resynchronize the microgrid with the frequency, amplitude, and phase of the grid in order to reconnect the microgrid to the grid seamlessly.

V. UPS INVERTER CONTROL

The control of the UPS inverter is based on three control loops [14]: 1) the inner voltage and current regulation loops; 2) the intermediate virtual impedance loop; and 3) the outer active and reactive-power-sharing loops. The inner voltage and current regulation loops can be implemented by using a conventional PI multiloop control or generalized integrators.

The virtual output impedance loop is able to fix the output impedance of the inverter by subtracting a processed portion of the output current i_o to the voltage reference of the inverter V_{ref} [13]. The output impedance for each current harmonic has been programmed by using a discrete Fourier transformation, as follows [15]:

$$V^* = V_{\text{ref}} - s \sum_{\text{odd}}^{h=N} L_{Vh} \cdot i_{oh} \tag{14}$$

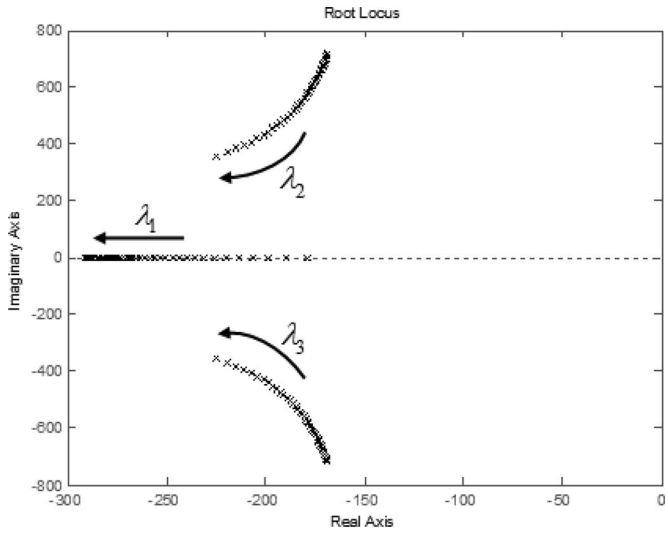

Fig. 4. Root-locus plot in function of the batteries charge level (arrows indicate decreasing values from 1 to 0.01).

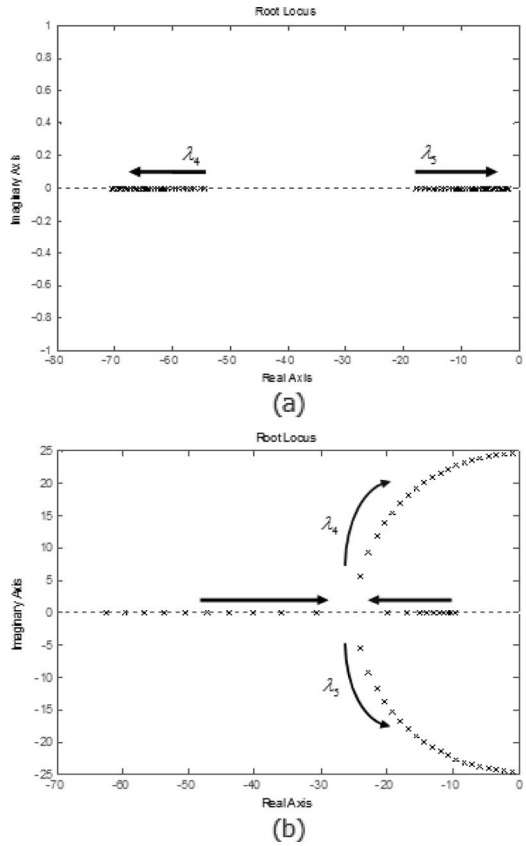

Fig. 5. Root-locus plot for (a) $k_p = 0.8$ and $0.1 \leq k_i \leq 0.8$. (b) $k_i = 0.5$ and $0.7 \leq k_p \leq 0.8$.

where V^* is the voltage reference of the inner control loops, i_{oh} is the hth harmonic current, and L_{Vh} is the impedance associated with each component. The output impedance of each harmonic can be adjusted to share properly the load currents but without greatly increasing the voltage total harmonic distortion (THD). Moreover, a hot-swap operation, i.e., the connection of more UPS modules without causing large current disturbances,

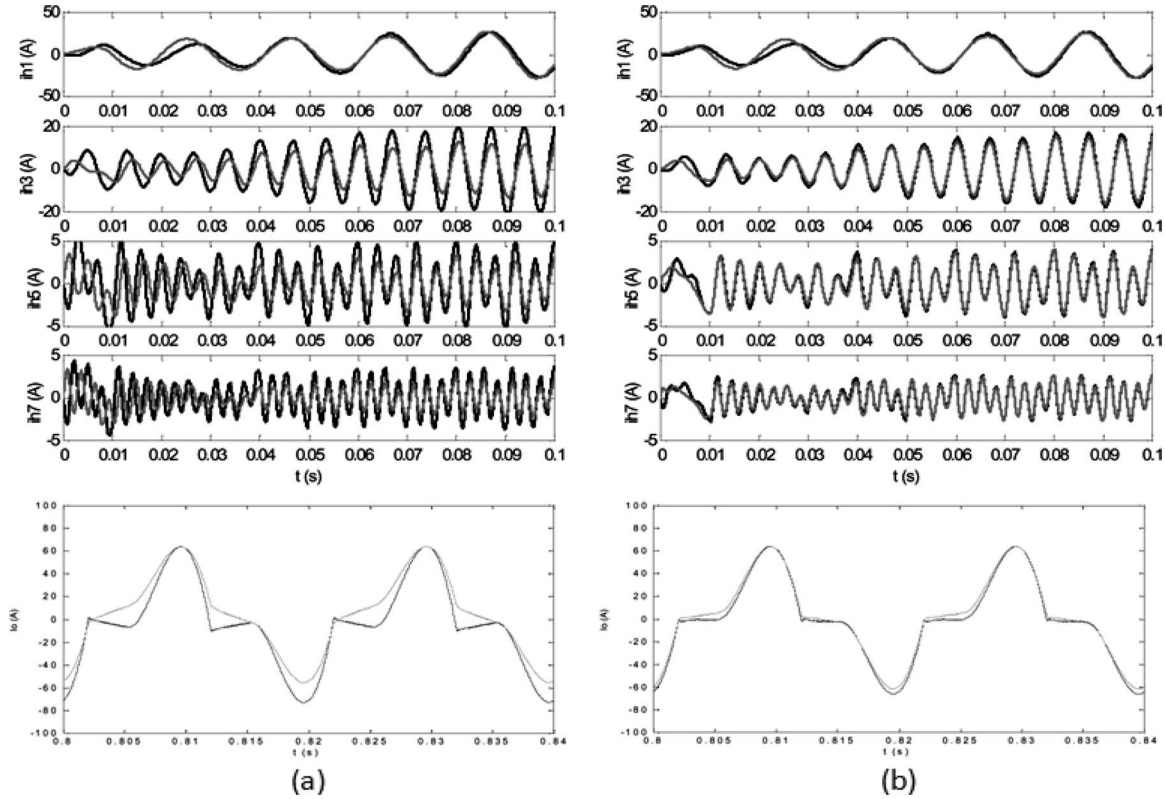

Fig. 6. Harmonic decomposition extracted by using the (top) bank of bandpass filters and (bottom) output currents of a two-UPS system with highly unbalanced power lines, sharing a nonlinear load (a) without and (b) with the harmonic-current sharing loop.

can be achieved by using a soft-start virtual impedance. The soft start is achieved by programming a high output impedance at the inverter connection to the microgrid. After the connection, the output impedance is then reduced slowly to a nominal value. This operation can be described by

$$L_V = L^*_{Df} + \left(L^*_{Do} - L^*_{Df}\right) \cdot e^{-t/T_{st}} \tag{15}$$

where L^*_{Do} and L^*_{Df} are the initial and final values of the output impedance and T_{st} is the time constant of the soft-start operation.

Once the output impedance is fixed, the droop method can operate properly. In the droop equations, derivative terms have been included to improve the transient response of the system [19]

$$\omega = \omega^* - m(P - P^*) - m_d \frac{d(P - P^*)}{dt} \tag{16}$$

$$E = E^* - n(Q - Q^*) - n_d \frac{d(Q - Q^*)}{dt} \tag{17}$$

where m_d and n_d are, respectively, the active and reactive derivative droop coefficients.

Fig. 3 shows the block diagram of the control loops of one inverter connected to the microgrid, including the inner current and voltage loops; the virtual impedance loop (14) with soft start (15); and the power-sharing loops (16) and (17).

VI. Small-Signal Analysis

A small-signal analysis is proposed to investigate the stability and transient response of the system. In order to ensure stability, a similar analysis as in [20] has been done, which results in a third-order system.

A. Primary Control Analysis

The closed-loop system dynamics is derived by considering the well-known stiff load-bus approximation [17]. The small-signal dynamics of the active and reactive powers, i.e., ΔP and ΔQ, respectively, are obtained by linearizing (5) and (6) and modeling the low-pass filters with a first-order approximation, i.e.,

$$\begin{pmatrix} \Delta P \\ \Delta Q \end{pmatrix} = \frac{\omega_c}{s + \omega_c} \frac{V}{X} \begin{pmatrix} \cos\Phi & -E\sin\Phi \\ \sin\Phi & E\cos\Phi \end{pmatrix} \begin{pmatrix} \Delta e \\ \Delta\phi \end{pmatrix} \tag{18}$$

where Δe denotes perturbed values; capital letters mean equilibrium point values; X is the output impedance at the fundamental frequency; and ω_c is the cutoff angular frequency of the low-pass filters, which are fixed over one decade below the line frequency. For simplicity, the high-frequency impedance values are not considered in this analysis since they have little effect

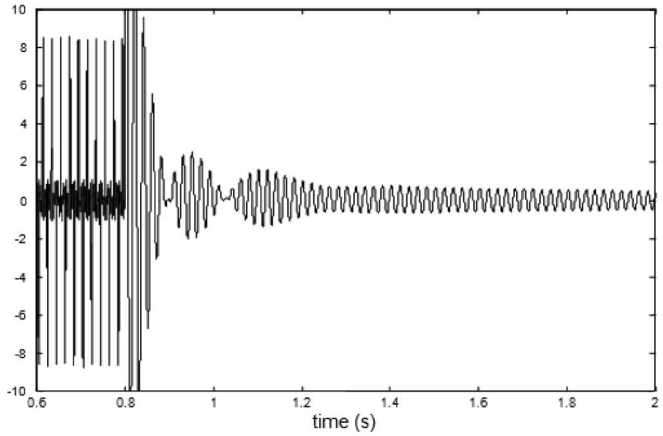

(a)

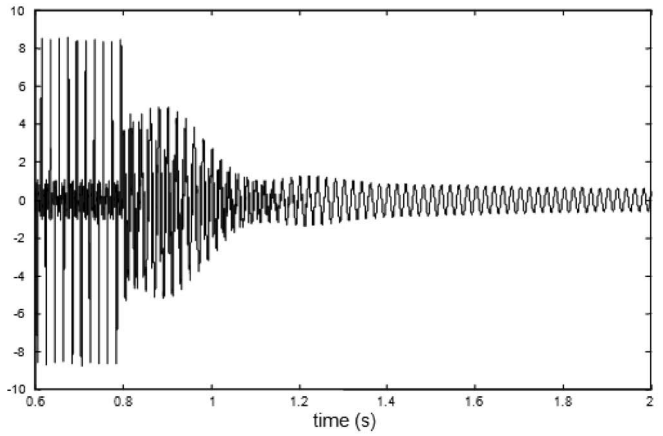

(b)

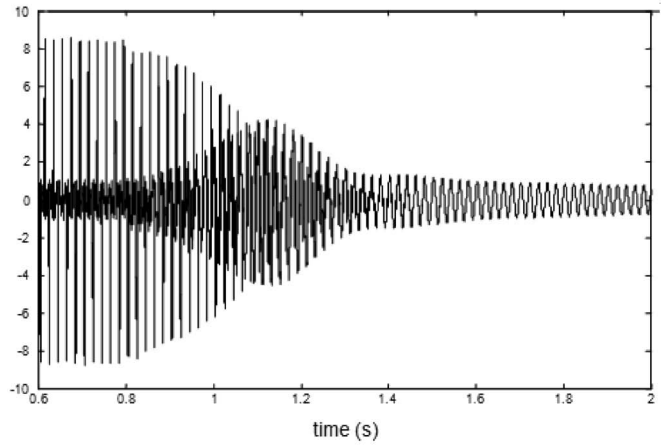

(c)

Fig. 7. Circulating current when a second UPS is connected at $t = 0.8$ (a) without the soft start, (b) with the soft start $L_{Do} = 80\ \mu$H, and (c) $L_{Do} = 800\ \mu$H (Y-axis: 2 A/div).

over the system dynamics. Subsequently, by perturbing (16) and (17) and using (18), we obtain

$$\Delta e = -(n + n_d s)\frac{\omega_c}{s + \omega_c}\frac{V}{R_d}[\cos\Phi \cdot \Delta e - E\sin\Phi \cdot \Delta\phi] \tag{19}$$

$$\Delta\phi = -\left(\frac{m}{s} + m_d\right)\frac{V \cdot \omega_c}{R_d(s + \omega_c)}[\sin\Phi \cdot \Delta e - E\cos\Phi \cdot \Delta\phi]. \tag{20}$$

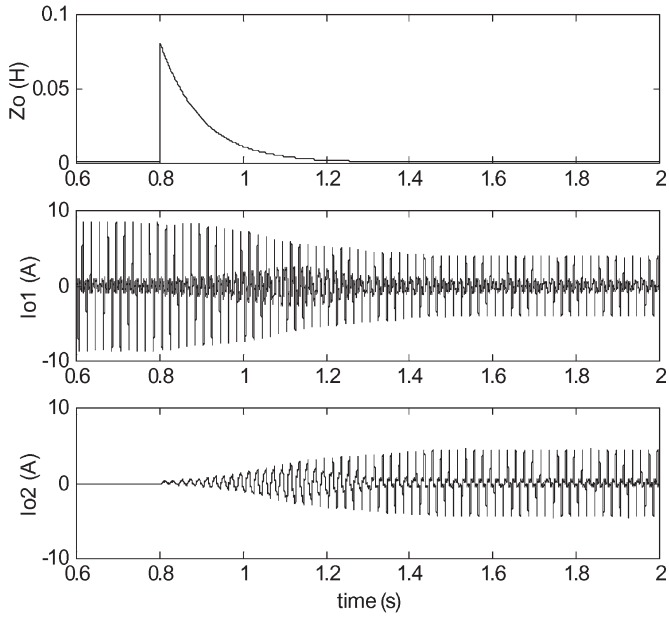

Fig. 8. Output impedance of UPS#2 and output currents of the UPS#1 and UPS#2 in soft-start operation ($T_{\rm ST} = 0.1$ s and $L_{Do} = 80\ \mu$H).

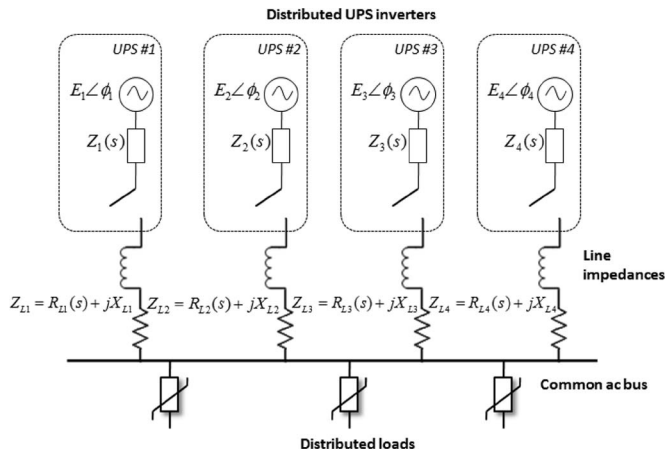

Fig. 9. Configuration setup for simulation results of the microgrid.

Finally, substituting (19) into (20), we can find a third-order small-signal dynamics of the closed-loop system

$$s^3 + As^2 + Bs + C = 0 \tag{21}$$

where

$$A = \frac{\omega_c}{X}\left[2R_D + nV\cos\Phi + n_d\omega_c V\cos\Phi + m_d VE\left(\cos\Phi + n_d\omega_c\frac{V}{X}\right)\right] \tag{22}$$

$$B = \frac{\omega_c}{X}\left[w_c + n\omega_c V\cos\Phi + mVE\cos\Phi + n_d\omega_c\frac{V}{X} + m_d\omega_c VE\left(\cos\Phi + n\frac{V}{X}\right)\right] \tag{23}$$

$$C = \frac{\omega_c}{X_d}m\omega_c VE\left(\cos\Phi + n\frac{V}{X}\right) \tag{24}$$

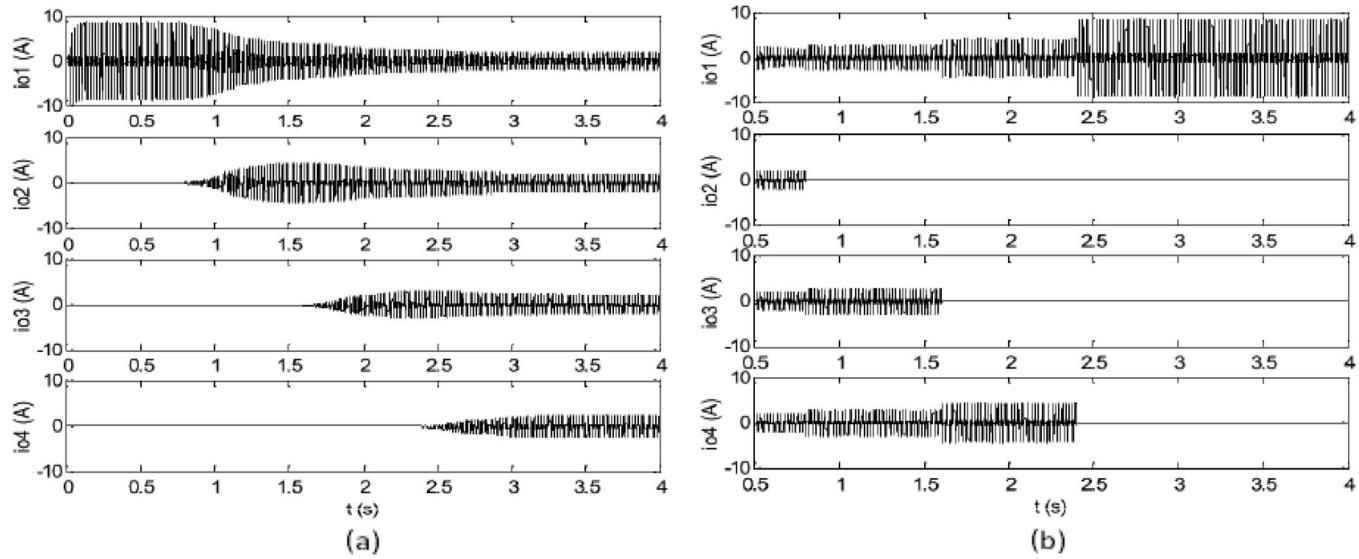

Fig. 10. Output currents of the UPS#1, UPS#2, UPS#3, and UPS#4 in (a) soft-start operation ($T_{\rm ST} = 0.1$ s and $L_{Do} = 80$ mH) and (b) disconnection scenario.

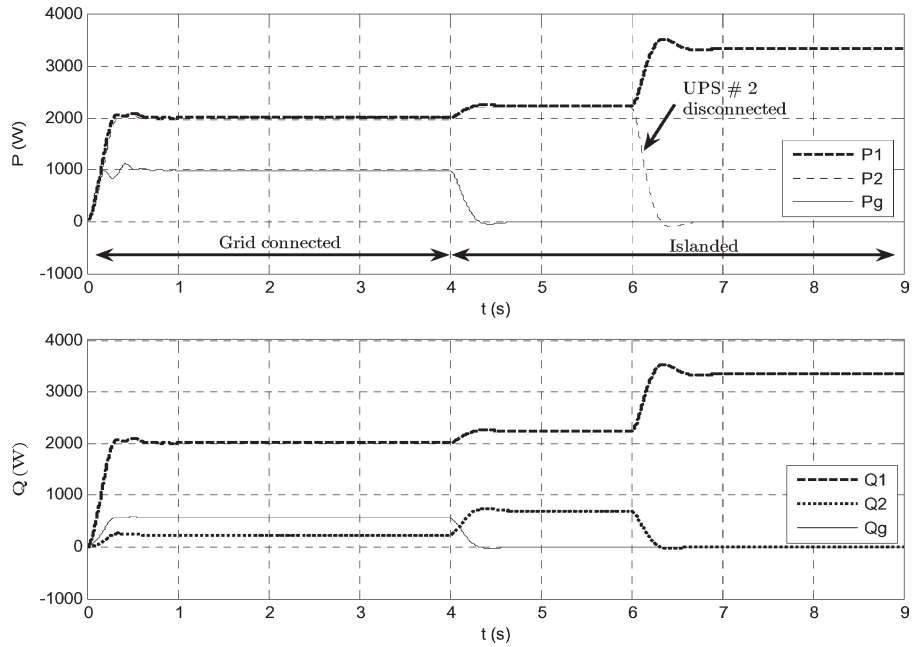

Fig. 11. Active- and reactive-power transients between grid-connected and islanded modes (Y-axis: $P = 1$ kW/div, $Q = 1$ kVAr/div).

with $X_d = X + n_d \omega_c V \cos\Phi$. Using (21), the stability of the closed-loop system can be evaluated, and the transient response can be adjusted. The eigenvalues of the system (λ_1, λ_2, and λ_3) have been studied by using the power stage and control parameters shown in Table I. Fig. 4 shows the family of root locus, showing stability for all battery charge conditions (from $\alpha = 1$ to $\alpha = 0.01$).

B. Secondary Control Analysis

Secondary control has been analyzed and modeled using a similar approach as in the last section. By using (7) and assuming a P/Q decoupling, the active power, given by one inverter, can be derived as

$$P_i = \frac{-m \cdot (P^* - P_i^*)\, EV\omega_c}{X(s + \omega_c)} \tag{25}$$

where P_i is the active power of the inverter i and P_i^* is the nominal active power. Combining (11) and (25) yields the following second-order transfer function:

$$\frac{P_i}{P_g^*} = \frac{(k_i + k_p s) mEV\omega_c / N}{Xs^2 + \omega_c \left[X + mEV(nk_p - 1)\right] s + NmEV\omega_c k_i}. \tag{26}$$

By studying the eigenvalues of (26), a series of root-locus diagrams is shown in Fig. 5(a) and (b), illustrating the stability limits which can be useful for adjusting the transient response of the system. A similar study can be done for reactive-power secondary control (12).

VII. Simulation and Experimental Results

The aim of this section is to test the proposed controller over the microgrid in order to show its performance and limitations in different scenarios.

A. Harmonic-Current Sharing

The first step is to observe the effect of the proposed controller over the harmonic-current sharing, which is very important when the system is supplying a nonlinear load. With this objective, a series of simulations have been performed for a two-UPS paralleled system sharing a common nonlinear load. Fig. 6(a) shows the steady-state and the transient responses of the inverters' output currents without using the harmonic sharing loop. In consequence, fundamental currents are equal; however, the third, fifth, and seventh harmonics are unbalanced. However, as shown in Fig. 6(b), by using (14), with the harmonic-current sharing loop, fundamental and harmonic-current terms are properly shared. Note that in this case, up to the seventh harmonic has been included. However, higher harmonics can be added to this control loop, if necessary.

B. Hot-Swap Operation

The second step consisted in testing the hot-swap operation of the UPS by using the proposed soft-start impedance. Two main scenarios must be considered, namely, the connection and the disconnection of the UPS in the distributed system. In the first case, when an additional UPS has to be connected to the common bus, the output voltage of the inverter must be synchronized with the bus by a phase-locked loop action. After that, the droop control method begins operating, together with the output impedance loop. As stated earlier, at first, the output impedance has a high value; later, however, it goes down to the nominal value in a soft-start fashion, avoiding initial current peaks.

Fig. 7 shows the circulating current $(i_{o1} - i_{o2})$ between two UPSs sharing a nonlinear load, when UPS#2 is connected at $t = 0.8$ s and while UPS#1 remains connected from the beginning. Fig. 7(a) shows the transient response of the circulating current without using the soft-start impedance, thus maintaining the L constant at 800 μH. Notice that the circulating current is initially higher than the current supplied by UPS#1 before the UPS#2 connection. Fig. 7(b) shows the transient response using the same configuration but adding the soft-start loop (15) with the following parameters: $T_{\rm ST} = 0.1$ s and $L = 80$ μH. Note that, in this case, the circulating current has been reduced by half. Fig. 7(c) shows the dynamic behavior of the circulating current by increasing L to 800 μH. Observe now that the system becomes slower while the initial current peak tends to increase.

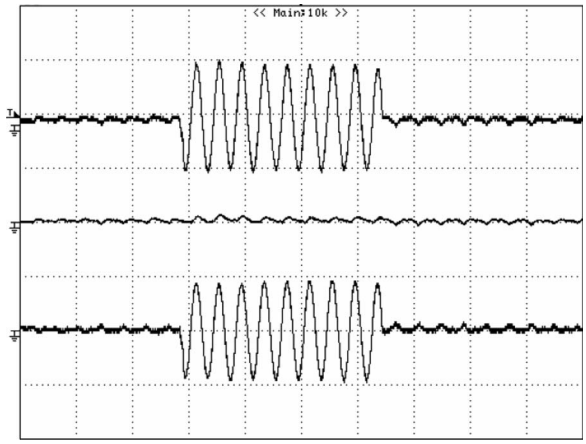

Fig. 12. Transient response of the output currents and the circulating current (X-axis: 50 ms/div; Y-axis: 20 A/div).

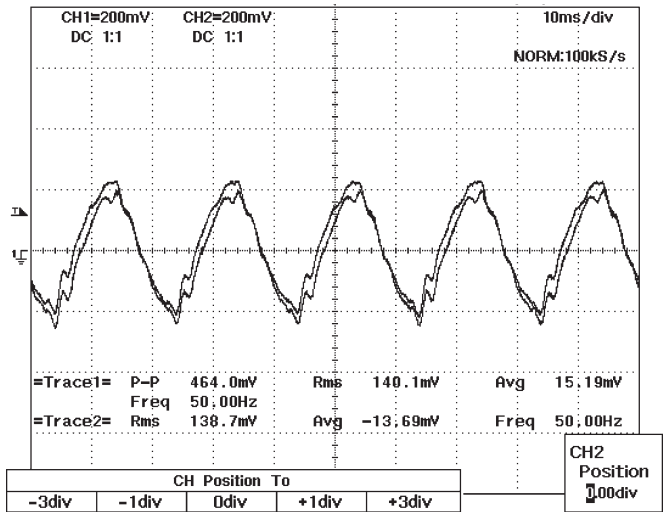

Fig. 13. Steady state of the output currents when sharing a pure 40-μF capacitive load (X-axis:10 ms/div; Y-axis: 5 A/div).

Fig. 8 shows a detail of the connection of UPS#2 while UPS#1 is connected to the load permanently. A four-UPS system sharing a distributed nonlinear load in order to see the effects of the inverter connection/disconnection has been simulated, and the results are shown in Fig. 10.

The impedances of the lines connected between the inverters and the load were intentionally unbalanced. $Z_{L1} = 0.12 + j0.028\Omega$, $Z_{L2} = 0.24 + j0.046\Omega$, $Z_{L3} = 0.06 + j0.014\Omega$, and $Z_{L4} = 0 + j0\Omega$ (see Fig. 9). Fig. 10(a) shows the progressive connection of the four UPSs to the common ac bus, with UPS#1 at $t = 0$ s, UPS#2 at $t = 0.8$ s, UPS#3 at $t = 1.6$ s, and UPS#4 at $t = 2.4$ s. As it can be seen, the UPS modules are seamlessly connected to the bus, increasing their output currents gradually. Fig. 10(b) shows the disconnection of the UPS from the ac bus. Note that there are no overcurrents. Droop functions for every UPS accommodate properly the output currents to the amount of load without critical transients.

C. Microgrid Operation and Transitions

Fig. 11 shows the active and reactive powers of a two-UPS microgrid sharing power with the grid, the transition to islanded

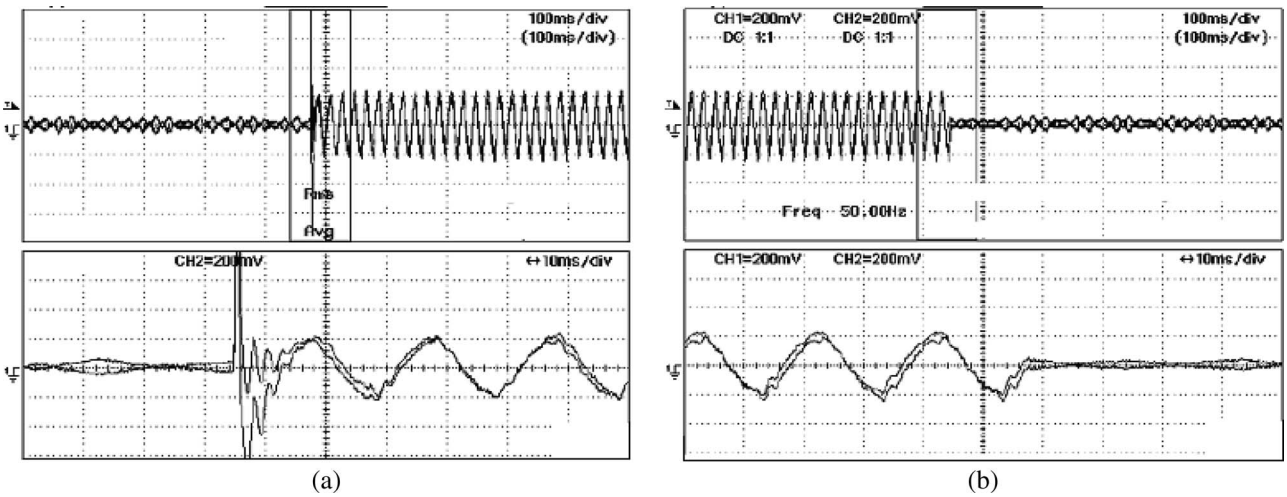

(a) (b)

Fig. 14. Dynamic performance of the output currents when sharing a pure 40-μF capacitive load. (a) Connection. (b) Disconnection (Y-axis: 4 A/div).

operation, and the disconnection of UPS#2. The system starts to be connected to the grid, with $P_g^* = 1000$ W and $Q_g^* = 0$ Var. At $t = 4$ s, the system is disconnected from the grid, and the two UPS units operate in island mode sharing the overall load. At $t = 6$ s, UPS#2 is disconnected, and UPS#1 supplies all the power to the microgrid. Notice the proper transient response, as well as the good power regulation of the system.

D. Experimental Results

Two 6-kVA single-phase UPS units were built and tested in order to show the validity of the proposed approach. Each inverter consisted of a single-phase insulated-gate bipolar transistor full bridge with a switching frequency of 20 kHz and an LC output filter, with the following parameters: $L = 500$ μH, $C = 100$ μF, $V_{\rm in} = 400$ V, and $V_o = 220$ $V_{\rm rms}$ at 50 Hz. The impedance of the lines connected between the inverters and the load was intentionally unbalanced; $Z_{L1} = 0.12 + j0.028\Omega$, and $Z_{L2} = 0.24 + j0.046\Omega$. The controls for these inverters are formed by three loops, namely, an inner current loop, an outer PI controller that ensures voltage regulation, and the power-sharing controller. The first two loops were implemented by means of a TMS320LF2407A fixed-point 40-MHz digital signal processor (DSP) from Texas Instruments. The power-sharing controller was implemented by using a TMS320C6711 floating-point 200-MHz DSP. The connection between the two DSPs was made through the host port interface of the '6711. This solution was used only in the design process. Afterward, within the developing process, we use a single fixed-point DSP TMS320C2811 as a controller. Thus, the cost and complexity of the control board are further reduced.

The DSP controller also includes a PLL block in order to synchronize the inverter with the common bus. In this situation, the static bypass switch is turned on, and the soft-start operation and the droop-based control are initiated. The first set of experiments considers a resistive load.

Fig. 12 shows the output currents of every unit and the circulating current $(i_{o1} - i_{o2})$ for sudden changes from no load to full load and vice versa. These results show an excellent dynamic response for the proposed controller. As it can be seen,

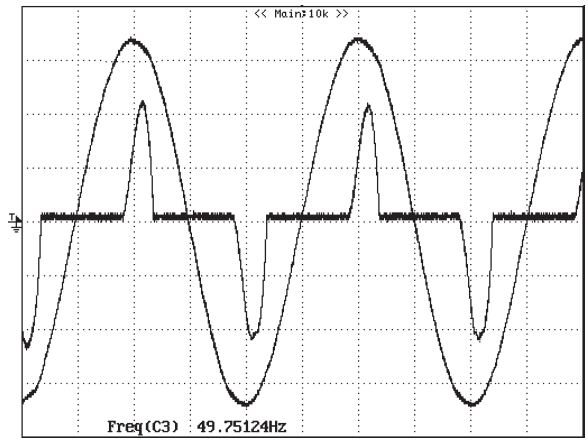

Fig. 15. Waveforms of the parallel system sharing a nonlinear load. Output voltage and load current (X-axis: 5 ms, Y-axis: 20 A/div).

the circulating current remains very small, even for no-load conditions. Furthermore, the supply of a purely capacitive load of 40 μF is evaluated. Figs. 13 and 14 show the steady-state and the transient responses of the output currents, respectively. The sudden connection of the capacitor to the ac bus causes a high current peak during the instantaneous charge process [see Fig. 14(a)]. The nonsinusoidal waveforms of these currents appear since the pure capacitive load compromises the performance of the inner voltage control loop.

As it can be seen, the proposed control achieves a good load-sharing capability in the system. The final experiment consists in supplying a nonlinear load. Fig. 15 shows the load voltage and current. The measured output voltage THD was about 2.1%.

VIII. Conclusion

In this paper, a control scheme for parallel-connected UPS systems forming a microgrid was proposed. The control structure of this paper was based on the droop method in order to achieve autonomous operation of each UPS module and how the droop method can be easily adaptable to the operation of parallel inverters. Moreover, the proposed control strategy

allows for achieving a tight P and Q regulation performance. A small-signal model was developed to analyze the system stability and to design the values of the control parameters. Experimental results have been presented in order to validate the proposed control approach, showing a good steady-state regulation and a proper transient response when sharing linear and nonlinear loads.

REFERENCES

[1] K. Alanne and A. Saari, "Distributed energy generation and sustainable development," *Renew. Sustain. Energy Rev.*, vol. 10, no. 6, pp. 539–558, Dec. 2006.

[2] R. H. Lasseter, A. Akhil, C. Marnay, J. Stevens, J. Dagle, R. Guttromson, A. S. Meliopoulous, R. Yinger, and J. Eto, "Integration of distributed energy resources: The CERTS microgrid concept," Consortium Elect. Reliab. Technol. Solutions, Berkeley, CA, pp. 1–27, Apr. 2002.

[3] P. L. Villeneuve, "Concerns generated by islanding," *IEEE Power Energy Mag.*, vol. 2, no. 3, pp. 49–53, May/Jun. 2004.

[4] M. C. Chandorkar and D. M. Divan, "Control of parallel connected inverters in standalone AC supply systems," *IEEE Trans. Ind. Appl.*, vol. 29, no. 1, pp. 136–143, Jan./Feb. 1993.

[5] C. C. Hua, K. A. Liao, and J. R. Lin, "Parallel operation of inverters for distributed photovoltaic power supply system," in *Proc. IEEE PESC*, 2002, pp. 1979–1983.

[6] S. Barsali, M. Ceraolo, P. Pelachi, and D. Poli, "Control techniques of dispersed generators to improve the continuity of electricity supply," in *Proc. IEEE PES—Winter Meeting*, 2002, vol. 2, pp. 789–794.

[7] M. N. Marwali, J. W. Jung, and A. Keyhani, "Control of distributed generation systems—Part II: Load sharing control," *IEEE Trans. Power Electron.*, vol. 19, no. 6, pp. 1551–1561, Nov. 2004.

[8] J. A. P. Lopes, C. L. Moreira, and A. G. Madureira, "Defining control strategies for microgrids islanded operation," *IEEE Trans. Power Syst.*, vol. 21, no. 2, pp. 916–924, May 2006.

[9] A. L. Dimeas and N. D. Hatziargyriou, "Operation of a multiagent system for microgrid control," *IEEE Trans. Power Syst.*, vol. 20, no. 3, pp. 1447–1455, Aug. 2005.

[10] F. D. Kanellos, A. I. Tsouchnikas, and N. D. Hatziargyriou, "Microgrid simulation during grid-connected and islanded modes of operation," presented at the Int. Conf. Power Systems Transients (IPST), Montreal, QC, Canada, 2005, Paper IPST05-113.

[11] Y. Zoka, H. Sasaki, N. Yorino, K. Kawahara, and C. C. Liu, "An interaction problem of distributed generators installed in a microgrid," in *Proc. IEEE DRPT*, 2004, pp. 795–799.

[12] M. Prodanovic and T. C. Green, "High quality power generation through distributed control of power park microgrid," *IEEE Trans. Ind. Electron.*, vol. 53, no. 5, pp. 1471–1482, Oct. 2006.

[13] J. M. Guerrero, L. G. de Vicuña, J. Matas, M. Castilla, and J. Miret, "Output impedance design of parallel-connected UPS inverters with wireless load-sharing control," *IEEE Trans. Ind. Electron.*, vol. 52, no. 4, pp. 1126–1135, Aug. 2005.

[14] J. M. Guerrero, L. G. de Vicuña, J. Matas, M. Castilla, and J. Miret, "A wireless controller to enhance dynamic performance of parallel inverters in distributed generation systems," *IEEE Trans. Power Electron.*, vol. 19, no. 5, pp. 1205–1213, Sep. 2004.

[15] J. M. Guerrero, J. Matas, L. G. de Vicuña, M. Castilla, and J. Miret, "Wireless-control strategy for parallel operation of distributed generation inverters," *IEEE Trans. Ind. Electron.*, vol. 53, no. 5, pp. 1461–1470, Oct. 2006.

[16] A. Tuladhar, H. Jin, T. Unger, and K. Mauch, "Control of parallel inverters in distributed ac power systems with consideration of line impedance effect," *IEEE Trans. Ind. Appl.*, vol. 36, no. 1, pp. 131–138, Jan./Feb. 2000.

[17] A. R. Bergen, *Power Systems Analysis*. Englewood Cliffs, NJ: Prentice-Hall, 1986.

[18] M. C. Chandorkar, D. M. Divan, Y. Hu, and B. Barnajee, "Novel architectures and control for distributed UPS systems," in *Proc. IEEE APEC*, 1994, pp. 683–689.

[19] J. M. Guerrero, J. Matas, L. G. de Vicuña, M. Castilla, and J. Miret, "Decentralized control for parallel operation of distributed generation inverters using resistive output impedance," *IEEE Trans. Ind. Electron.*, vol. 54, no. 2, pp. 994–1004, Apr. 2007.

[20] E. A. Coelho, P. C. Cortizo, and P. F. Garcia, "Small signal stability for single phase inverter connected to stiff AC system," in *Conf. Rec. 34th IEEE IAS Annu. Meeting*, 1999, vol. 4, pp. 2180–2187.

[21] J. M. Guerrero, N. Berbel, J. Matas, J. L. Sosa, and L. G. de Vicuña, "Control of line-interactive UPS connected in parallel forming a microgrid," in *Proc. IEEE ISIE*, 2007, pp. 2667–2672.

[22] J. C. Vásquez, J. M. Guerrero, E. Gregorio, P. Rodríguez, R. Teodorescu, and F. Blaabjerg, "Adaptive droop control applied to distributed generation inverters connected to the grid," in *Proc. IEEE ISIE*, 2008, pp. 2420–2425.

[23] J. M. Guerrero, L. García de Vicuña, and J. Uceda, "Uninterruptible power supply systems provide protection," *IEEE Ind. Electron. Mag.*, vol. 1, no. 1, pp. 28–38, Spring 2007.

[24] J. M. Guerrero, L. Hang, and J. Uceda, "Control of distributed uninterruptible power supply systems," *IEEE Trans. Ind. Electron.*, vol. 55, no. 8, pp. 2845–2859, Aug. 2008.

[25] M. Arias, A. Fernandez, D. G. Lamar, M. Rodriguez, and M. M. Hernando, "Simplified voltage-sag filler for line-interactive uninterruptible power supplies," *IEEE Trans. Ind. Electron.*, vol. 55, no. 8, pp. 3005–3011, Aug. 2008.

[26] H. Tao, J. L. Duarte, and M. A. M. Hendrix, "Line-interactive UPS using fuel cell as the primary source," *IEEE Trans. Ind. Electron.*, vol. 55, no. 8, pp. 3005–3011, Aug. 2008.

[27] Z. He and Y. Xing, "Distributed control for UPS modules in parallel operation with RMS voltage regulation," *IEEE Trans. Ind. Electron.*, vol. 55, no. 8, pp. 2860–2869, Aug. 2008.

[28] M. Pascual, G. Garcerá, E. Figueres, and F. González-Espín, "Robust model-following control of parallel UPS single-phase inverters," *IEEE Trans. Ind. Electron.*, vol. 55, no. 8, pp. 2870–2883, Aug. 2008.

[29] K.-S. Low and R. Cao, "Model predictive control of parallel-connected inverter for uninterruptible power supplies," *IEEE Trans. Ind. Electron.*, vol. 55, no. 8, pp. 2860–2869, Aug. 2008.

[30] M. Castilla, J. Miret, J. Matas, L. Garcia de Vicuna, and J. M. Guerrero, "Linear current control scheme with series resonant harmonic compensator for single-phase grid-connected photovoltaic inverters," *IEEE Trans. Ind. Electron.*, vol. 55, no. 7, pp. 2724–2733, Jul. 2008.

[31] L. R. Chen, N. Y. Chu, C. S. Wang, and R. H. Liang, "Design of a reflex-based bidirectional converter with the energy recovery function," *IEEE Trans. Ind. Electron.*, vol. 55, no. 8, pp. 3022–3029, Aug. 2008.

[32] Y. C. Chuang and Y. L. Lee, "High-efficiency and low-stress ZVT–PWM DC-to-DC converter for battery charger," *IEEE Trans. Ind. Electron.*, vol. 55, no. 8, pp. 3030–3037, Aug. 2008.

Josep M. Guerrero (S'01–M'04–SM'08) received the B.S. degree in telecommunications engineering, the M.S. degree in electronics engineering, and the Ph.D. degree in power electronics from the Technical University of Catalonia, Barcelona, Spain, in 1997, 2000, and 2003, respectively.

He is an Associate Professor with the Department of Automatic Control Systems and Computer Engineering, Technical University of Catalonia, Barcelona, where he currently teaches courses on digital signal processing, control theory, microprocessors, and renewable energy. Since 2004, he has been responsible for the Renewable Energy Laboratory, Escola Industrial de Barcelona, Barcelona. His research interests include photovoltaics, wind energy conversion, uninterruptible power supplies, storage energy systems, and microgrids.

Dr. Guerrero is the Editor-in-Chief of the *International Journal of Integrated Energy Systems*. He is also an Associate Editor for the IEEE TRANSACTIONS ON INDUSTRIAL ELECTRONICS, the IEEE TRANSACTIONS ON POWER ELECTRONICS, the *International Journal of Power Electronics*, and the *International Journal of Industrial Electronics* and *Drives*.

Juan C. Vásquez received the B.S. degree in electronics engineering from the Universidad Autónoma de Manizales, Manizales, Colombia, in 2004. Currently, he is working toward the Ph.D. degree in the Department of Automatic Control Systems and Computer Engineering, Technical University of Catalonia, Barcelona, Spain.

He was an Assistant Professor with the Universidad Autónoma de Manizales, where he taught courses on digital circuits, servo systems, and flexible manufacturing systems. His research interests include modeling, simulation, and management applied to distributed generation in microgrids.

José Matas received the B.S., M.S., and Ph.D. degrees in telecommunications engineering from the Technical University of Catalonia, Barcelona, Spain, in 1988, 1996, and 2003, respectively.

From 1988 to 1990, he was with an electronic equipment company, as an Engineer. Since 1990, he has been an Associate Professor with the Department of Electronic Engineering, Technical University of Catalonia, Vilanova i la Geltrú, Spain. His research interests include power factor correction circuits, active-power filters, uninterruptible power systems, distributed power systems, and nonlinear control.

Miguel Castilla received the B.S., M.S., and Ph.D. degrees in telecommunications engineering from the Technical University of Catalonia, Barcelona, Spain, in 1988, 1995, and 1998, respectively.

Since 2002, he has been an Associate Professor with the Department of Electronic Engineering, Technical University of Catalonia, Vilanova i la Geltrú, Spain, where he teaches courses on analog circuits and power electronics. His research interests are in the areas of power electronics, nonlinear control, and renewable energy systems.

Luis García de Vicuña received the M.S. and Ph.D. degrees in telecommunication engineering from the Technical University of Catalonia, Barcelona, Spain, in 1980 and 1990, respectively, and the Ph.D. degree in power electronics from the Université Paul Sabatier, Toulouse, France, in 1992.

From 1980 to 1982, he was an Engineer with a control applications company. He is currently an Associate Professor with the Department of Electronic Engineering, Technical University of Catalonia, Vilanova i la Geltrú, Spain, where he teaches courses on power electronics. His research interests include power electronics modeling, simulation and control, active-power filtering, and high-power-factor ac/dc conversion.